Neoplasia • Vol. 8, No. 7, July 2006, pp. 534–542

www.neoplasia.com

Activity of the Vascular-Disrupting Agent 5,6-Dimethylxanthenone-4-Acetic Acid against Human Head and Neck Carcinoma Xenografts[1]

Mukund Seshadri, Richard Mazurchuk†, Joseph A. Spernyak†, Arup Bhattacharya†, Youcef M. Rustum† and David A. Bellnier**

Departments of *Cell Stress Biology (Photodynamic Therapy Center) and †Cancer Biology (Preclinical Imaging Resource), Roswell Park Cancer Institute, Buffalo, NY 14263, USA

Abstract

Head and neck squamous cell carcinomas (HNSCC) constitute a majority of the tumors of the upper aerodigestive tract and continue to present a significant therapeutic challenge. To explore the potential of vascular-targeted therapy in HNSCC, we investigated the antivascular, antitumor activity of the potent vascular-disrupting agent (VDA) 5,6-dimethylxanthenone-4-acetic acid (DMXAA) against two HNSCC xenografts with markedly different morphologic and vascular characteristics. Athymic nude mice bearing subcutaneous FaDu (human pharyngeal squamous cell carcinoma) and A253 (human submaxillary gland epidermoid carcinoma) tumors were administered a single dose of DMXAA (30 mg/kg, i.p). Changes in vascular function were evaluated 24 hours after treatment using contrast-enhanced magnetic resonance imaging (MRI) and immunohistochemistry (CD31). Signal enhancement (*E*) and change in longitudinal relaxation rates (ΔR_1) were calculated to measure alterations in vascular perfusion. MRI showed a 78% and 49% reduction in vascular perfusion in FaDu and A253 xenografts, respectively. CD31-immunostaining of tumor sections revealed three-fold (FaDu) and two-fold (A253) reductions in microvessel density (MVD) 24 hours after treatment. DMXAA was equally effective against both xenografts, with significant tumor growth inhibition observed 30 days after treatment. These results indicate that DMXAA may be beneficial in the management of HNSCC, alone or in combination with other treatments.
Neoplasia (2006) **8,** 534–542

Keywords: Head and neck cancers, DMXAA, tumor vasculature, MRI, antivascular therapies.

Introduction

Head and neck squamous cell carcinomas (HNSCC) represent more than 90% of all head and neck cancers, with ~37,000 new cases reported annually in the United States [1,2]. A majority of the patients with early-stage disease are treated with either surgery or radiation [3]. Management of patients with locoregional advanced disease typically includes the use of cytotoxic chemotherapeutic agents [3,4]. However, clinical response rates of HNSCC have remained relatively unchanged over the years, especially in patients with recurrent or metastatic disease, highlighting the need for a multidisciplinary therapeutic approach [3,4]. Clinical studies have often focused on improving antitumor activity by combining therapies that target multiple tumor pathways [5]. Recent randomized clinical trials have also demonstrated increased response rates with combination strategies compared to those with single-agent therapies [5,6].

To grow, solid tumors need nutrients and oxygen supplied by blood vessels [7]. As such, selective targeting of established tumor vasculature represents an attractive anticancer strategy [8], and a number of vascular-disrupting agents (VDAs) are being actively pursued in research and clinical settings [9]. 5,6-Dimethylxanthenone-4-acetic acid (DMXAA) is one such potent VDA that has been shown to possess excellent antitumor activity against transplanted murine tumors [10,11] and xenografts [11–15]. Biologic response to DMXAA is a result of direct drug effects on endothelial cells and of indirect effects mediated by cytokines such as tumor necrosis factor α [16]. Vascular effects of DMXAA are usually seen within a few hours after administration and include changes in vascular permeability that lead to plasma loss, increased blood viscosity, intravascular thrombosis, and eventual loss of blood flow within the tumor [16]. Several studies have reported the effects of DMXAA in human tumor xenograft models, including melanomas [11], colorectal cancer [12], ovarian cancer [11,13], breast cancer [13], prostate cancer [14], and lung cancer [15]. However, the antitumor activity of DMXAA against HNSCC

Abbreviations: VDA, vascular-disrupting agent; HNSCC, head and neck squamous cell carcinomas; DMXAA, 5,6-dimethylxanthenone-4-acetic acid; MR, magnetic resonance; MVD, microvessel density

Address all correspondence to: David A. Bellnier, Department of Cell Stress Biology and the Photodynamic Therapy Center, Roswell Park Cancer Institute, Elm and Carlton Streets, Buffalo, NY 14263. E-mail: david.bellnier@roswellpark.org

[1]This work was supported by National Institutes of Health grant R01CA89656 (D.A. Bellnier). This work used core facilities supported, in part, by Roswell Park Cancer Institute's National Cancer Institute–funded Cancer Center Support Grant CA16056.
Received 13 April 2006; Revised 31 May 2006; Accepted 31 May 2006.

DOI 10.1593/neo.06295

has not been previously investigated. We therefore evaluated the antivascular and antitumor effects of DMXAA using two HNSCC xenografts, FaDu (human pharyngeal squamous cell carcinoma) and A253 (human submaxillary gland epidermoid carcinoma), that have been previously shown to vary in morphologic characteristics, vascularity, and response to irinotecan therapy [17]. The objectives of the study were to determine if: 1) the vascular responses of the two xenografts to DMXAA were different; 2) long-term tumor response rates were different; and 3) the observed early alterations in vascular function were predictive of treatment outcome. The effects of DMXAA on tumor vasculature were evaluated using noninvasive magnetic resonance imaging (MRI) and immunohistochemical staining of tumor sections for the endothelial cell adhesion molecule (CD31). Tumor response was determined by monitoring tumor growth for a period of 30 days following treatment.

Materials and Methods

HNSCC Xenografts

The human head and neck carcinoma lines FaDu [18] and A253 [19] were originally purchased from the American Type Culture Collection (Manassas, VA). The xenografts were initially established by subcutaneously injecting 10^6 cells into athymic nude mice. For experiments, visibly non-necrotic tumor pieces obtained from donor mice were transplanted into the flanks of 12-week-old female athymic nude mice (*nu/nu*; Harlan Sprague Dawley, Inc., Indianapolis, IN), as described previously [20]. Studies were performed when tumors were approximately 5 to 7 mm in diameter.

DMXAA

Solid DMXAA (courtesy of Gordon Rewcastle, University of Auckland, Auckland, New Zealand) was stored at room temperature in the dark and dissolved in 0.5% sodium bicarbonate immediately before intraperitoneal injection at a dose of 30 mg/kg.

MR Contrast-Enhancing Agent

Albumin-GdDTPA [21] (courtesy of Robert Brasch) was obtained from Contrast Media Laboratory, Department of Radiology, University of California at San Francisco (San Francisco, CA). This agent has been extensively characterized and used for experimental studies [22,23]. The agent contains 35 GdDTPA molecules (94.3 mM) that are bound to each human serum albumin (2.69 mM). T_1 relaxivity was calculated to be 11.3 mM^{-1} sec^{-1} per Gd ion at 25°C and 10 MHz.

Contrast-Enhanced MRI

Mice were imaged using a 4.7-T/33-cm horizontal bore magnet (GE NMR Instruments, Fremont, CA) incorporating AVANCE digital electronics [Bruker Biospec, ParaVision 3.0.2 (OS); Bruker Medical, Billerica, MA], a removable gradient coil insert (G060; Bruker Medical) generating a maximum field strength of 950 mT/m, and a custom-designed radiofrequency transreceiver coil. Animals were anesthetized before imaging with a ketamine/xylazine mixture (10:1) at a dose of 1.0 ml/100 mg, secured in a mouse coil chamber, and positioned on a scanner. The animals were kept warm in the magnet using a circulating water bath maintained at 37°C. Data acquisition consisted of a localizer, T_1-weighted MR images, and T_2-weighted MR images. Anatomic coverage included the tumor, kidneys, and muscles. In addition, a signal-to-noise calibration standard (phantom containing a known concentration of contrast agent) was placed in the field of view (FOV) to normalize signal intensity (SI) values obtained from different animals over time. A series of three preliminary noncontrast-enhanced images, with repetition times (T_R) ranging from 360 to 6000 milliseconds, was acquired before an intravenous bolus injection of the contrast agent for the determination of regional precontrast T_1 relaxation values. Following these baseline acquisitions, albumin-GdDTPA (0.1 mmol/kg) was introduced manually through tail vein injection, and a second series of five postcontrast images was serially obtained for ~45 minutes (day 1), as described previously [22,23]. T_1 relaxation rates were determined using a saturation recovery, fast spin echo sequence with an effective echo time (T_E) of 10 milliseconds, and a T_R ranging from 360 to 6000 milliseconds [FOV = 32 × 32 mm, slice thickness = 1.0 mm, matrix size = 128 × 96 pixels, number of excitations (N_{EX}) = 3]. Following image acquisition, animals were allowed to recover, and 30 mg/kg DMXAA was injected intraperitoneally in a volume of 0.2 ml of 0.5% sodium bicarbonate in distilled water. Twenty-four hours after DMXAA administration, a second set of images was acquired with an identical imaging protocol as that on day 1. The mice then received a second injection of albumin-GdDTPA at the same dose, and imaging was performed for ~45 minutes after contrast agent administration, as before. On completion of image acquisitions, mice were humanely sacrificed, and tumors were excised for immunohistochemistry and histology. All procedures were carried out in accordance with protocols approved by the RPCI Institutional Animal Care and Use Committee.

Image Processing and Data Analysis

Image processing and analysis were carried out using commercially available software (ANALYZE PC, Version 5.0; Biomedical Imaging Resource, Mayo Foundation, Rochester, MN) (Matlab's curve-fitting toolbox, Matlab Version 7.0; Math Works, Inc., Natick, MA) and source codes developed by the RPCI Preclinical Imaging Resource. Regions of interest (ROI) of tumors, kidneys, and muscle tissues were manually drawn in the images and object maps of the ROI constructed. SI values from different ROI were obtained and used to calculate tumor enhancement (E) [22,23]. SI values were corrected for temporal variation in the spectrometer by normalizing to the phantom. Percent tumor enhancement (E) was then calculated from relative intensity (RI)

$$RI = SI_{tumor}/SI_{phantom}$$

in precontrast and postcontrast images and reported as percent enhancement using the formula

$$E = [(RI_{post} - RI_{pre})/RI_{pre}] \times 100\%$$

Tumor T_1 relaxation rates ($R_1 = 1 / T_1$) were calculated from serially acquired images obtained before and after the administration of albumin-GdDTPA. Precontrast and postcontrast R_1 values were calculated as previously described [24]. To calculate DMXAA-induced changes in vascular volume and permeability, the change in longitudinal relaxation rate ΔR_1 was calculated over time by subtracting the average precontrast R_1 value from each of the five serially acquired postcontrast R_1 measurements. ΔR_1 values were reported as a function of time before and after DMXAA treatment. The slope of the ΔR_1 series was used as a measure of vascular permeability, and *Y*-intercept was used to estimate vascular volume, similar to the method described previously by Bhujwalla *et al.* [25].

Immunohistochemical Analysis of Microvessel Density (MVD)

Tumors were excised and immediately placed in Tris-buffered zinc fixative (BD Biosciences Pharmingen, San Diego, CA) overnight, transferred to 70% ethanol, dehydrated, and embedded in paraffin. Sections 5 μm thick were stained after conventional deparaffinization, endogenous peroxidase quenching with 3% H_2O_2, and pretreatment with 0.03% casein in phosphate-buffered saline (PBS) with 500 μl/l Tween for 30 minutes at room temperature to block unspecific binding. Slides were counterstained with Harris hematoxylin (Poly Scientific, Bayshore, NY). Mouse CD31 was detected with rat monoclonal antibody (IgG2a; BD Biosciences Pharmingen) at 1:50 dilution in PBS for 60 minutes at 37°C. This was followed by the addition of biotinylated rabbit anti-rat IgG (12112D; Biosciences Pharmingen) at 1:100 dilution for 30 minutes, streptavidin peroxidase (50-242; Zymed, San Francisco, CA) for 30 minutes, and diaminobenzidine for 5 minutes [17,26]. An isotype-matched control (10 μg/ml rat IgG) was used on a duplicate slide in place of the primary antibody as a negative control. Intratumoral blood vessels were counted on cross sections of whole tumor under the high-power field (HPF) of a light microscope (original magnification, ×400). Two to three sections from the center of each tumor were used to determine the average number of microvessels per field. Vessels with a clearly defined lumen or a well-defined linear vessel shape were counted. Single endothelial cells were not counted as vessels.

Tumor Response

Following treatment, tumors were measured with vernier calipers every 1 to 3 days for a period of 30 days, and tumor volumes were calculated using the formula $1 / 2(LW^2)$, where *L* is the longest tumor axis. Actual tumor volume (ATV) calculated on different days after treatment was normalized to initial tumor volume (ITV) on the day of treatment and was reported as: median tumor volume % [(ATV / ITV) × 100]. Tumor cure percentages are reported either as complete response (CR) when no tumor was detected by palpation or as partial response (PR) when tumor volume was temporarily reduced by 50% [17].

Statistics

All measured values are reported as mean ± standard error of the mean. Three animals were used for MRI studies for each tumor type. For immunohistochemistry, four to five animals were used for control and DMXAA treatment groups. Five to eight animals per group were used for tumor response studies. Two-tailed *t* test and one-way analysis of variance were used for comparing individual treatment groups with controls. $P = .05$ was considered statistically significant. All statistical calculations and analyses were performed using Graph Pad Prism (Version 4.00; Graph Pad, San Diego, CA).

Results

Differences in Vascular Perfusion between Untreated FaDu and A253 Xenografts

We have recently shown that A253 tumors consisted of 30% avascular regions and 70% poorly vascularized regions (MVD = 10 per ×400 HPF), whereas FaDu tumors had a higher (MVD = 19 per ×400) and more homogeneous distribution of microvessels [17]. Although both xenografts responded to the chemotherapeutic agent irinotecan, the greater resistance of A253 *vs* FaDu was attributed to inadequate drug uptake in the avascular and poorly vascularized regions of A253 tumors.

To confirm these differences in tumor vasculature before therapy with the antivascular and antitumor drug DMXAA, percent enhancement (*E*) in MR signal intensity following contrast agent administration was calculated in untreated control tumors. As expected the enhancement values (indicative of tumor tissue vascularity) were significantly different ($P < .05$) between these tumors (Figure 1), with FaDu xenografts exhibiting an approximately three-fold greater enhancement than A253 tumors (82.04 ± 14.53 *vs* 27.24 ± 6.60, respectively). To further validate vascular differences between the two xenografts, quantitative estimates of vascular perfusion were obtained from ΔR_1 values calculated following contrast agent administration. As seen in Figure 2, a significant difference ($P < .001$) in ΔR_1 was seen between

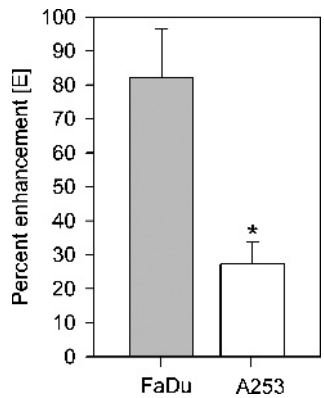

Figure 1. *Vascular differences between FaDu and A253 xenografts. Graph shows percent enhancement (E) in MR signal intensity following contrast agent administration in FaDu and A253 human HNSCC implanted subcutaneously in nude mice (two-tailed Student's t test, *P < .05).*

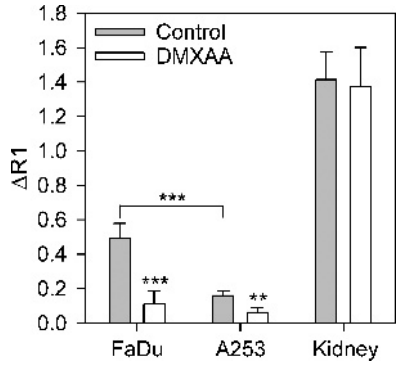

Figure 2. *Vascular response of tumor and kidney tissues to DMXAA. Change in T_1 relaxation rates (ΔR_1) of control and DMXAA-treated FaDu and A253 tumors calculated from serial T_1-weighted MR images acquired before and 24 hours after administration of albumin-GdDTPA. The ΔR_1 values of kidneys before and 24 hours after DMXAA treatment are included. Values represent mean ± SEM (two-tailed Student's t test, ***P < .001, **P < .01, *P < .05).*

untreated FaDu and A253 xenografts. These measured differences in vascularity between FaDu and A253 are summarized in Table 1.

Vascular Responses of FaDu and A253 Xenografts to DMXAA

The vascular responses of FaDu and A253 xenografts were studied using albumin-GdDTPA contrast-enhanced MRI following administration of 30 mg/kg DMXAA. Change in longitudinal relaxation rate (ΔR_1) following contrast agent administration was calculated 24 hours after DMXAA treatment and was compared to pretreatment values. As seen in Figure 2, there was a difference between the two xenografts in the degree of vascular response to DMXAA. Twenty-four hours after treatment, FaDu tumors exhibited a 78% reduction ($P < .001$) in ΔR_1 (0.109 ± 0.005) compared to baseline values (0.494 ± 0.053), indicative of a substantial decrease in vascular perfusion. In contrast, A253 tumors exhibited a 49% reduction ($P < .01$) in ΔR_1 following DMXAA (0.148 ± 0.012 and 0.076 ± 0.012) before and after treatment respectively. To assess the effects of DMXAA on normal tissue, ΔR_1 values were calculated in the kidneys before and after DMXAA treatment. As can be seen in Figure 2, no significant change in ΔR_1 was seen in the kidneys as a result of DMXAA treatment. Additionally, no difference was seen in R_1 values calculated from a reference muscle tissue (data not shown) before and 24 hours after DMXAA treatment.

To further characterize the differences in vascular response between the two tumors, ΔR_1 values were calculated over time (~45 minutes) following contrast agent administration. These ΔR_1 values were then plotted as a function of time, and parameters of vascular volume (*Y*-intercept) and permeability (slope) were calculated. A linear increase in ΔR_1 was seen in both FaDu and A253 tumors before treatment, reflecting an accumulation of contrast agent (Figure 3). As seen before, the vascular volume of control FaDu (0.297 ± 0.014) tumors was significantly higher ($P < .0001$) than that of A253 tumors (0.102 ± 0.003) before DMXAA treatment. Following DMXAA treatment, there was a highly significant ($P < .0001$) three-fold reduction in the vascular volume of FaDu tumors (*Y*-intercept = 0.090 ± 0.002), indicative of significant DMXAA-induced vascular damage. Analysis of the two slopes also revealed significant differences ($P < .001$), suggestive of alterations in permeability as a result of impaired perfusion following DMXAA treatment. Analysis of ΔR_1 values of A253 tumors over time revealed a moderate, but statistically insignificant, change (1.3-fold, $P = .154$) in vascular volume following DMXAA treatment; there was a small difference between the slopes of the ΔR_1 value−time plots, but it was not statistically significant ($P = .143$).

We then investigated if parameters of vascular function determined by MRI correlated with histologic estimates of MVD. To achieve this, immunohistochemical staining of tumor sections was performed for the pan endothelial cell adhesion molecule, CD31. Figure 4 shows histologic [hematoxylin and eosin (H&E)] and immunohistochemical (CD31) sections of control and DMXAA-treated FaDu and A253 tumors. Histological section of untreated control FaDu tumors showed uniformly poorly differentiated tumor cells (*panel A*), with evenly distributed blood vessels as defined by their positive CD31 immunoreactivity (*panel B*). Blood vessels appeared as distinct clusters of endothelial cells with intact lumen (*arrows*). Following DMXAA treatment, extensive necrosis and hemorrhaging (*panel C*) were seen in FaDu tumors, with marked loss of vessel integrity, a virtual absence of CD31 staining (*panel D*), and the presence of cellular congestion inside vessel lumens (*arrows*). Control A253 tumors showed well-differentiated tumor regions (*panel E*) with fewer blood vessels (*panel F*, *arrows*). DMXAA-treated A253 tumor sections also showed necrosis and hemorrhage (*panel G*), with considerable loss of CD31 immunostaining and intravascular congestion (*panel H*, *arrows*).

MVD was calculated by an analysis of control and DMXAA-treated tumor sections for CD31-positive blood

Table 1. Summary of Histologic and Vascular Characteristics of Untreated HSNCC Xenografts and Tumor Response Rates Following a Single Treatment of DMXAA.

Tumor Type	Histologic Characteristics*	MVD†	% Enhancement (*E*)‡	ΔR_1‡	CR Rate (%)§
FaDu	Uniformly poorly differentiated	20.75 ± 1.87	82.04 ± 14.53	0.494 ± 0.053	20
A253	30% Avascular and well-differentiated; 70% poorly differentiated	9.67 ± 1.33	27.24 ± 6.60	0.148 ± 0.012	20

*Bhattacharya et al. [17].
†Immunostaining of tumor sections with anti-CD31 antibody.
‡Contrast-enhanced MRI.
§Percent tumor-free mice.

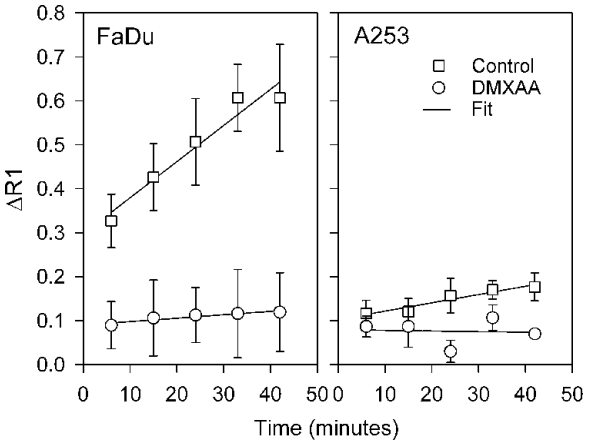

Figure 3. *Change in vascular volume and permeability following DMXAA. Graph shows change in T_1 relaxation rates (ΔR_1) over time of untreated control tumors (squares) and tumors treated with 30 mg/kg DMXAA (circles) for FaDu (left panel) and A253 (right panel) xenografts. Vascular volume and permeability values were calculated from ΔR_1 using linear regression analysis. Significant differences were seen between the vascular volumes (Y-intercepts) of control FaDu and control A253 xenografts ($P < .0001$). Twenty-four hours after treatment, only FaDu tumors exhibited a significant reduction in vascular volume versus control ($P < .0001$). Analysis of the slopes of the plots also revealed a significant difference in permeability between control and DMXAA-treated FaDu tumors ($P < .001$).*

vessels in multiple HPFs (Figure 5). The results showed that the MVDs of control FaDu and A253 tumors were considerably different ($P < .01$), consistent with MR findings. A significant decrease in MVD ($P < .01$ for FaDu and $P < .05$ for A253) was seen in both tumor sections (Figure 5), in agreement with MR findings.

To visualize the differences in vascular responses between FaDu and A253 xenografts, T_1 relaxation maps (Figure 6, *maps B*, *D*, *F*, and *H*) were computed. Representative proton images are also shown (Figure 6, *images A*, *C*, *E*, and *G*). In the figure, *images A*, *B*, *C*, and *D* were obtained before DMXAA treatment, and *images E*, *F*, *G*, and *H* were acquired 24 hours after treatment. As seen in the figure, before the DMXAA treatment, both tumors show increased MR signal enhancement following contrast agent administration (*map D*), with FaDu tumors (*yellow arrows*) exhibiting greater enhancement than A253 tumors (*white arrows*). Twenty-four hours after DMXAA treatment, no detectable MR signal enhancement was seen in FaDu tumors following contrast agent administration (*map H*) compared to precontrast images (*map F*). At the same time point, A253 showed enhancement following treatment, indicating the presence of functional vessels (*maps F* and *H*).

Tumor Growth Inhibition of FaDu and A253 Xenografts by DMXAA

We have shown that DMXAA reduced mean vessel density and vascular perfusion to different degrees in FaDu and A253 xenografts. To test the effects of DMXAA on tumor growth, tumor-bearing mice were injected with a single dose (30 mg/kg) of DMXAA and monitored for a period of 30 days. This treatment resulted in significant ($P < .001$) inhibition of A253 and FaDu tumor growth relative to controls (Figure 7); however, there was no difference in posttreatment growth rates ($P > .05$) and cure rates (20%) between these two tumor lines.

Discussion

Head and neck cancer is the fifth most common malignancy worldwide and presents a significant challenge to clinicians [1,2]. Standard treatment options, such as surgery, radiation, or chemotherapy, or their combination, can result in tumor cures and preservation of organs and function in early-stage disease [3,4]. However, prognosis is poorer for patients with advanced disease, indicating the need for new therapeutic approaches [4–6].

The critical role of the vasculature in tumor growth and progression has generated a great deal of interest in drugs that either disrupt existing tumor vessels or prevent new vessel formation [7,8]. These vascular-targeted therapies exploit differences in vascular physiology between normal and tumor tissues [7,8]. Presently, a number of VDAs are being evaluated against different types of cancers in preclinical studies and on patients [9]. DMXAA is one such potent VDA that has been shown to induce selective tumor vascular shutdown and hemorrhagic necrosis in several murine models and xenografts [10–15]. We report here the response of two HNSCC xenografts, FaDu and A253, to a single dose of the VDA, DMXAA. Contrast-enhanced MRI and endothelial cell immunostaining describe the loss of vascular integrity and function after DMXAA, which results in significant inhibition of tumor growth 30 days after treatment.

In contrast to conventional anticancer therapies, VDAs such as DMXAA are not expected to result in dramatic changes in tumor size or volume [13,16]. In general, VDAs are believed to be more effective against vessels in the interior of the tumor, with a characteristic rim of cells in the periphery that remains viable after treatment [15,16]. Therapeutic assessment based on biomarkers [27] directly or indirectly related to their mechanism of action is therefore necessary, as traditional measures of response alone may not reflect their true biologic activity [16]. One such parameter that has been used in the assessment of tumor response to DMXAA in animal models and in patients is alteration in vascular perfusion [28,29]. In this regard, contrast-enhanced MRI has become an increasingly popular tool to monitor vascular function following treatment [28,30]. The noninvasive nature of MR, combined with its ability to sample the whole tumor, makes it ideal for monitoring the effect of vascular-targeted therapies [30]. Most contrast-enhanced MRI studies performed to date have used low-molecular-weight contrast agents that freely diffuse transendothelially and have a high first-pass extraction fraction to evaluate the response of tumors to antivascular treatments [30]. However, it is well-recognized that these low-molecular-weight contrast agents may not be particularly well suited for this purpose, as VDAs such as DMXAA are known to increase vascular permeability and result in reduction of tumor blood flow [16,31]. To avoid some of these complexities associated with pharmacokinetic modeling and MR data interpretation,

we have used a well-characterized intravascular agent albumin-GdDTPA to obtain quantitative estimates of vascular perfusion in the two HNSCC xenografts 24 hours after DMXAA treatment.

Previously, using contrast-enhanced MRI based on a macromolecular contrast agent that remained predominantly intravascular in untreated tumors, we have shown that DMXAA resulted in a significant increase in vascular

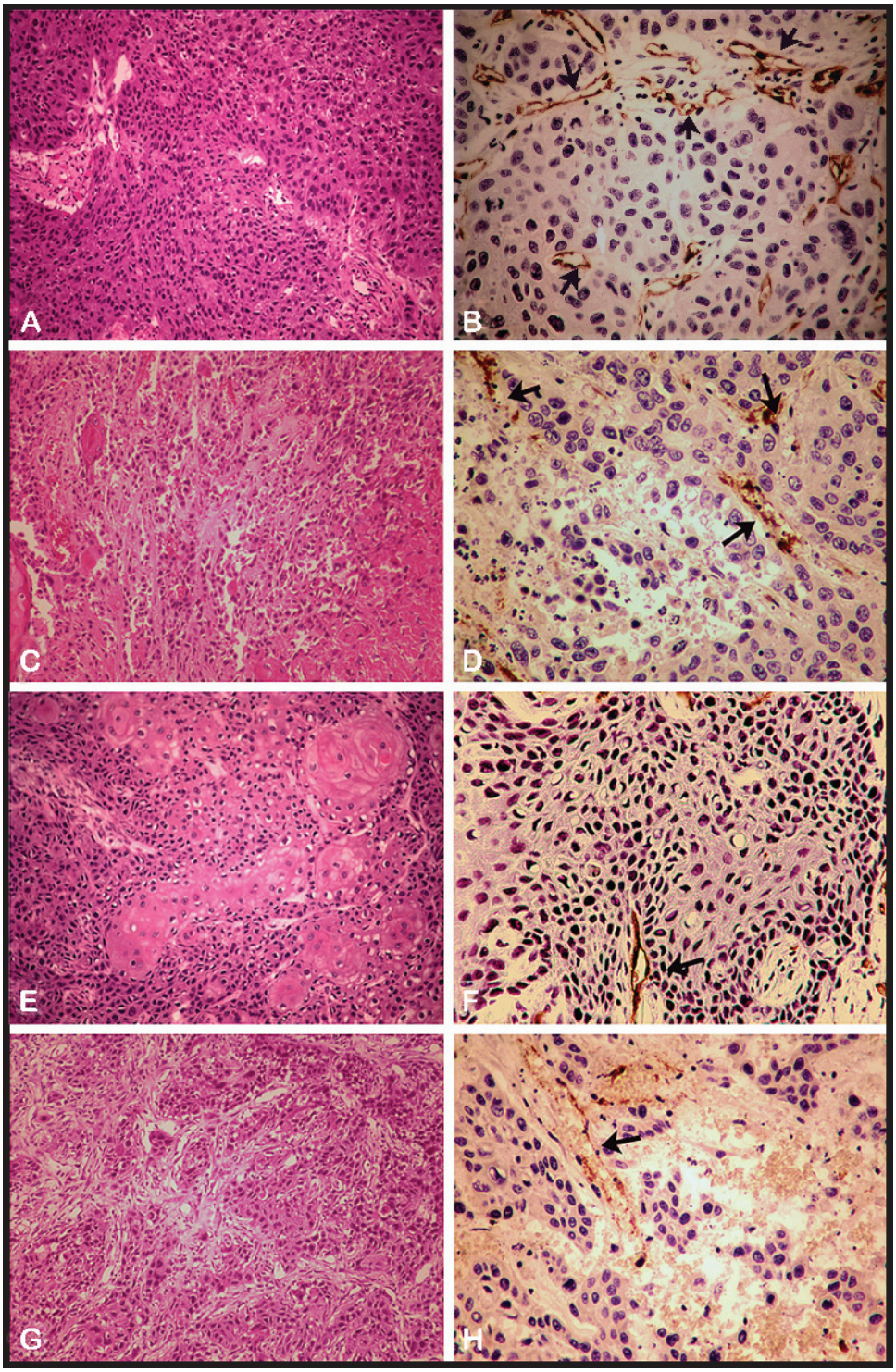

Figure 4. *Effect of DMXAA therapy on HNSCC xenografts. Photomicrographs of control and DMXAA-treated FaDu (upper two rows) and A253 (lower two rows) xenografts are shown before and 24 hours after DMXAA treatment. The left column shows H&E–stained tumor sections (original magnification, ×200), and the right column shows CD31-immunostained tumor sections (original magnification, ×400). Control FaDu xenografts consist of uniformly poorly differentiated regions (panel A) with increased MVD (panel B; arrows), whereas A253 tumors consist of hypoxic, avascular, well-differentiated islands (panel E) with fewer vessels (panel F; arrows). Twenty-four hours after DMXAA treatment, both FaDu (panel C) and A253 (panel G) tumors showed extensive necrosis and loss of CD31 staining (FaDu, panel D; A253, panel H) indicative of significant DMXAA-induced vascular damage (arrows).*

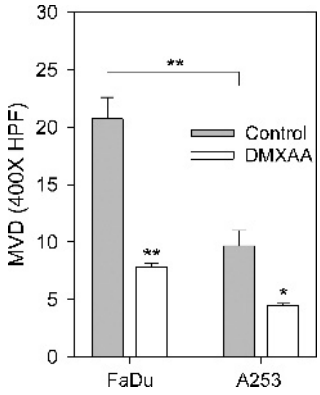

Figure 5. *Estimates of MVD in FaDu and A253 xenografts following DMXAA treatment. Bar graphs show MVD counts for control and DMXAA-treated FaDu and A253 tumors per HPF (original magnification, ×400). Significant reduction in MVD was seen 24 hours after DMXAA treatment (two-tailed Student's t test, **P < .01, *P < .05).*

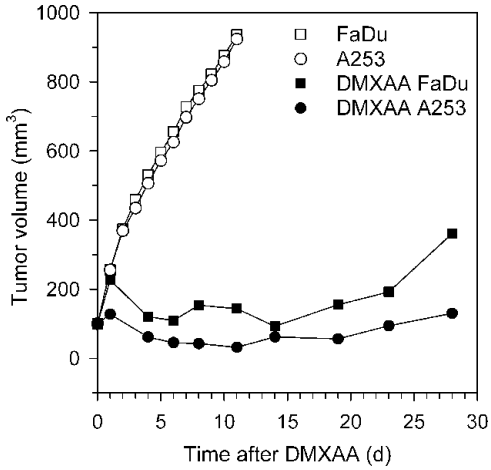

Figure 7. *Tumor growth inhibition following DMXAA. Nude mice bearing bilateral FaDu and A253 xenografts were injected with 30 mg/kg DMXAA, and tumor growth was monitored for a period of 30 days. Figure shows change in median tumor volume between DMXAA-treated tumors and untreated controls. DMXAA resulted in significant inhibition (P < .001) of the growth of both xenografts compared to untreated controls.*

permeability 4 hours after treatment in murine colon 26 tumors [24]. In the same study, in addition to an increase in permeability 4 hours after treatment, we also observed a significant reduction in R_1 values 24 hours after DMXAA treatment, indicative of significant alterations in vascular perfusion at this time. We therefore chose to examine vascular perfusion 24 hours after DMXAA treatment in the two HNSCC xenografts. We hypothesized that if DMXAA exhibited antivascular activity in the two xenografts, then vascular shutdown induced by the drug 24 hours after treatment would result in a decreased uptake of the contrast agent and therefore a decrease in the MR parameter (ΔR_1) measured. Changes in longitudinal relaxation rate [ΔR_1 ($R_1 = 1 / T_1$)] following administration of a contrast agent were evaluated before and 24 hours after treatment with DMXAA to provide quantitative measures of tumor vascular volume and permeability.

Our results show that DMXAA exhibits moderate antivascular and antitumor activity against both HNSCC xenografts used. MRI revealed significant vascular differences between untreated FaDu and A253 tumors (Figures 1 and 2), in agreement with our previous study [17]. Following DMXAA treatment, FaDu tumors exhibited a more dramatic reduction in vascular perfusion compared to A253 xenografts (Figures 2 and 3). This could be due to differences in the underlying histologic structures of these xenografts. FaDu tumors consist of uniformly poorly differentiated regions with higher MVD,

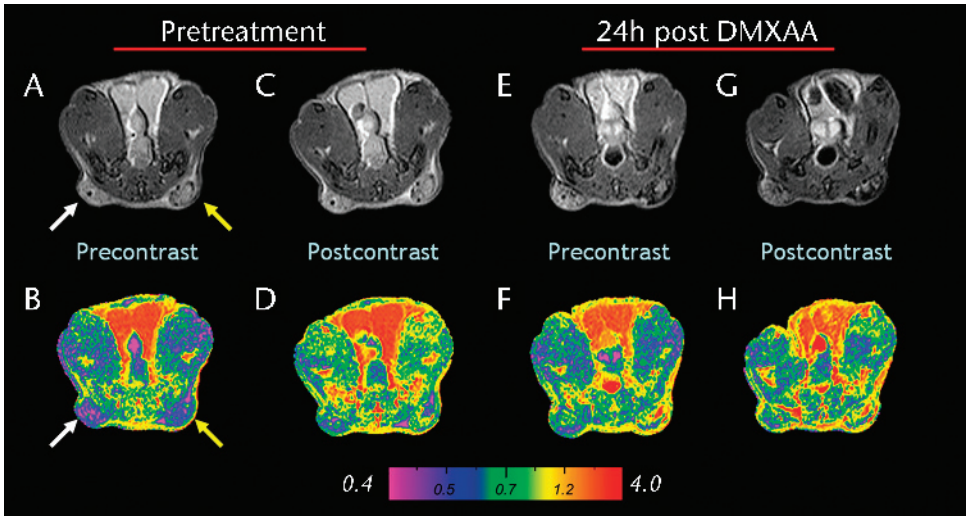

Figure 6. *Visualization of FaDu and A253 vascular response to DMXAA. T_1 relaxation maps (lower panel) of a nude mouse bearing bilateral FaDu (yellow arrows) and A253 (white arrows) xenografts. Maps (B) and (D) represent the precontrast and postcontrast images acquired before DMXAA treatment. Maps (F) and (H) represent the precontrast and postcontrast images acquired 24 hours after DMXAA treatment. Twenty-four hours after DMXAA treatment, no detectable MR signal enhancement was seen in FaDu tumors after contrast agent administration (map H) compared to precontrast images (map F). At the same time point, A253 showed enhancement, indicating the presence of functional vessels (maps F and H). Representative proton images are also shown (images A, C, E, and G).*

whereas A253 tumors consist of 30% well-differentiated avascular regions and 70% poorly differentiated regions with low MVD [17]. The tight cellular architecture of A253 tumors is also believed to hinder endothelial cell penetration and thereby prevent blood vessel formation [17]. This may have contributed to the differential response of the two xenografts, as vascular endothelial cells are the primary targets of VDAs, including DMXAA. Immunohistochemical staining (Figure 4) and MVD counts (Figure 5) correlated with MR findings and confirmed DMXAA-induced vascular damage. Differences in the vascular response between the two tumors were also visualized using contrast-enhanced MRI (Figure 6). Contrast-enhanced MRI also demonstrated the selectivity of antivascular effects of DMXAA, as normal muscles and kidney tissues did not show any significant change following treatment.

As summarized in Table 1, the histologic and vascular characteristics of the two HNSCC xenografts used were significantly different. Changes in MR parameters of vascular function were predictive of the long-term outcome observed following treatment. Although the vascular response to DMXAA was more dramatic in FaDu tumors compared to A253, tumor response studies demonstrated that DMXAA resulted in significant growth inhibition of both tumors compared to untreated controls (Figure 7). The observed differences in the degree of vascular response to DMXAA between the two tumors could have been a direct consequence of differences in their vascularity. Nevertheless, the moderate reduction in vascular perfusion seen in A253 following DMXAA treatment was still sufficient to produce a significant antitumor effect. Because A253 tumors are less vascularized to begin with, it could be that each vessel within the tumor supports many more tumor cells compared to FaDu tumors. Therefore, it is possible that the amount of tumor cell kill achieved by DMXAA-induced vascular damage is the same in A253 tumors as in FaDu tumors, accounting for the same CR rates (20%) in both tumor types (Table 1).

The CR rates (20%) seen in these xenografts are not completely surprising as VDAs such as DMXAA are not expected to cause significant growth delays as single agents [31]. The true clinical usefulness of agents such as DMXAA is believed to be in combination settings. Several preclinical studies have shown significant synergistic activity of DMXAA in combination with chemotherapy, radiation, and approaches such as hyperthermia and gene therapy [31]. We have previously shown that administration of a low ineffective dose of DMXAA significantly potentiates the antitumor activity and selectivity of photodynamic therapy [24, 26].

Here, we have demonstrated the potential for the clinical application of DMXAA in head and neck cancers. As such, clinical trials employing VDAs such as CA4P, in combination with radiotherapeutic and chemotherapeutic agents, are underway for the management of thyroid cancer (http://www.clinicatrials.gov; NCT00077103 and NCT00060242). Although the activity of vascular-targeting agents such as ZD6126 has been reported against HNSCC xenografts [32], to the best of our knowledge, no preclinical studies evaluating the effect of DMXAA against head and neck tumors have been published before this report. Taken together, DMXAA appears to be moderately effective against HNSCC and may be clinically useful in the management of head and neck cancers, either alone or in combination. However, it is important to keep in mind that these studies were carried out using implanted subcutaneous tumors and that the observed antivascular and antitumor effects of DMXAA may be reflective of the response of tumors beneath the skin rather than of orthotopic tumors. Systematic evaluation of the antitumor effects of DMXAA using orthotopic tumor models is therefore necessary to better understand its clinical potential. Studies aimed at addressing this issue are currently underway in our laboratory.

References

[1] Sanderson RJ and Ironside JAD (2002). Squamous cell carcinomas of the head and neck. *BMJ* **325,** 822–827.

[2] Jemal A, Murray T, Ward E, Samuels A, Tiwari RC, Ghafoor A, Feuer EJ, and Thun MJ (2005). Cancer statistics, 2005. *CA Cancer J Clin* **55,** 10–30.

[3] Seiwert TY and Cohen EE (2005). State-of-the-art management of locally advanced head and neck cancer. *Br J Cancer* **92,** 1341–1348.

[4] Cohen EE, Lingen MW, and Vokes EE (2004). The expanding role of systemic therapy in head and neck cancer. *J Clin Oncol* **22,** 1743–1752.

[5] Baselga J, Trigo JM, Bourhis J, Tortochaux J, Cortes-Funes H, Hitt R, Gascon P, Amellal N, Harstrick A, and Eckardt A (2005). Phase II multicenter study of the antiepidermal growth factor receptor monoclonal antibody cetuximab in combination with platinum-based chemotherapy in patients with platinum-refractory metastatic and/or recurrent squamous cell carcinoma of the head and neck. *J Clin Oncol* **23,** 5568–5577.

[6] Gibson MK, Li Y, Murphy B, Hussain MH, DeConti RC, Ensley J, Forastiere AA. Eastern Cooperative Oncology Group (2005). Randomized phase III evaluation of cisplatin plus fluorouracil *versus* cisplatin plus paclitaxel in advanced head and neck cancer (E1395): an intergroup trial of the Eastern Cooperative Oncology Group. *J Clin Oncol* **23,** 3562–3567.

[7] Folkman J (1971). Tumor angiogenesis: therapeutic implications. *N Engl J Med* **285,** 1182–1186.

[8] Denekamp J (1990). Vascular attack as a therapeutic strategy for cancer. *Cancer Metastasis Rev* **9,** 267–282.

[9] Thorpe PE (2004). Vascular targeting agents as cancer therapeutics. *Clin Cancer Res* **10,** 415–427.

[10] Rewcastle GW, Atwell GJ, Zhuang L, Baguley BC, and Denny WA (1991). Potential antitumor agents: 61. Structure–activity relationships for *in vivo* colon-38 activity among disubstituted 9-oxo-9*H*-xanthene-4-acetic acids. *J Med Chem* **34,** 217–222.

[11] Joseph WR, Cao Z, Mountjoy KG, Marshall ES, Baguley BC, and Ching L-M (1999). Stimulation of tumours to synthesize tumor necrosis factor-a *in situ* using 5,6-dimethylxanthenone-4-acetic acid: a novel approach to cancer therapy. *Cancer Res* **59,** 633–638.

[12] Pedley RB, Boden JA, Boden R, Boxer GM, Flynn AA, Keep PA, and Begent RH (1996). Ablation of colorectal xenografts with combined radioimmunotherapy and tumor blood flow–modifying agents. *Cancer Res* **56,** 3293–3300.

[13] Siemann DW, Mercer E, Lepler S, and Rojiani AM (2002). Vascular targeting agents enhance chemotherapeutic agent activities in solid tumor therapy. *Int J Cancer* **99,** 1–6.

[14] Green C, Griffiths-Johnson D, Dunmore KR, Robson M, Clark S, and Kelland LR (2005). Marked potentiation of the *in vivo* antitumor activity of docetaxel in a human prostate cancer xenograft by the vascular targeting agent 5,6 dimethyl xanthenone acetic acid, DMXAA. *Proc Am Assoc Cancer Res* **46,** 2990.

[15] Kelland LR (2005). Targeting established tumor vasculature: a novel approach to cancer treatment. *Curr Cancer Ther Rev* **1,** 1–9.

[16] Tozer GM, Kanthou C, and Baguley BC (2005). Disrupting tumor blood vessels. *Nat Rev Cancer* **5,** 423–435.

[17] Bhattacharya A, Tóth K, Mazurchuk R, Spernyak JA, Slocum HK, Pendyala L, Azrak R, Cao S, Durrani FA, and Rustum YM (2004). Lack of microvessels in well differentiated regions of human head and neck squamous cell carcinoma A253 is associated with fMR imaging

detectable hypoxia, limited drug delivery and resistance to irinotecan therapy. *Clin Cancer Res* **10,** 8005–8017.

[18] Rangan SR (1972). A new human cell line (FaDu) from a hypopharyngeal carcinoma. *Cancer* **29,** 117–121.

[19] Fogh J, Fogh JM, and Orfeo T (1977). One hundred and twenty-seven cultured human tumor cell lines producing tumors in nude mice. *J Natl Cancer Inst* **59,** 221–226.

[20] Cao S, Durrani FA, and Rustum YM (2004). Selective modulation of the therapeutic efficacy of anticancer drugs by selenium containing compounds against human tumor xenografts. *Clin Cancer Res* **10,** 2561–2569.

[21] Schmiedl U, Ogan M, Paajanen H, Marotti M, Crooks LE, Brito AC, and Brasch RC (1987). Albumin labeled with Gd-DTPA as an intravascular, blood pool–enhancing agent for MR imaging: biodistribution and imaging studies. *Radiology* **162,** 205–210.

[22] Schmiedl U, Ogan MD, Moseley ME, and Brasch RC (1986). Comparison of the contrast-enhancing properties of albumin-(Gd-DTPA) and Gd-DTPA at 2.0 T: and experimental study in rats. *Am J Roentgenol* **147,** 1263–1270.

[23] Aicher KP, Dupon JW, White DL, Aukerman SL, Moseley ME, Juster R, Rosenau W, Winkelhake JL, and Brasch RC (1990). Contrast-enhanced magnetic resonance imaging of tumor-bearing mice treated with human recombinant tumor necrosis factor alpha. *Cancer Res* **50,** 7376–7381.

[24] Seshadri M, Spernyak JA, Mazurchuk R, Camacho SH, Oseroff AR, Cheney RT, and Bellnier DA (2005). Tumor vascular response to photodynamic therapy and the antivascular agent 5,6-dimethylxanthenone-4-acetic acid: implications for combination therapy. *Clin Cancer Res* **11,** 4214–4250.

[25] Bhujwalla ZM, Artemov D, Natarajan K, Ackerstaff E, and Solaiyappan M (2001). Vascular differences detected by MRI for metastatic *versus* non-metastatic breast and prostate cancer xenografts. *Neoplasia* **3,** 143–153.

[26] Bellnier DA, Gollnick SO, Camacho SH, Greco WR, and Cheney RT (2003). Treatment with tumor necrosis factor-α–inducing 5,6-dimethylxanthenone-4-acetic acid enhances the antitumor activity of the photodynamic therapy of RIF-1 mouse tumors. *Cancer Res* **63,** 7584–7590.

[27] Biomarkers Definitions Working Group (2001). Biomarkers and surrogate endpoints: preferred definitions and conceptual framework. *Clin Pharmacol Ther* **69,** 89–95.

[28] Galbraith SM, Rustin GJ, Lodge MA, Taylor NJ, Stirling JJ, Jameson M, Thompson P, Hough D, Gumbrell L, and Padhani AR (2002). Effects of 5,6-dimethylxanthenone-4-acetic acid on human tumor microcirculation assessed by dynamic contrast-enhanced magnetic resonance imaging. *J Clin Oncol* **20,** 3826–3840.

[29] Beauregard DA, Pedley RB, Hill SA, and Brindle KM (2002). Differential sensitivity of two adenocarcinoma xenografts to the antivascular drugs combrestatin A4 phosphate and 5,6-dimethylxanthenone-4-acetic acid, assessed using MRI and MRS. *NMR Biomed* **15,** 99–105.

[30] Padhani AR and Leach MO (2005). Antivascular cancer treatments: functional assessments by dynamic contrast-enhanced magnetic resonance imaging. *Abdom Imaging* **30,** 324–341.

[31] Baguley BC and Wilson WR (2002). Potential for DMXAA combination therapy for solid tumors. *Expert Rev Anticancer Ther* **2,** 593–603.

[32] Davis PD, Dougherty GJ, Blakey DC, Galbraith SM, Tozer GM, Holder AL, Naylor MA, Nolan J, Stratford MR, Chaplin DJ, et al. (2002). ZD6126: a novel vascular-targeting agent that causes selective destruction of tumor vasculature. *Cancer Res* **62,** 7247–7253.